PROCEEDINGS OF SCIENCE

Flavour anomalies at LHCb

Georgios Chatzikonstantinidis[*†]
University of Birmingham, Birmingham, United Kingdom
E-mail: georgios.chatzikonstantinidis@cern.ch

Flavour-Changing Neutral-Current (FCNC) processes are exceptionally sensitive to New Physics (NP) effects and in particular to particles that could exist beyond the Standard Model (SM) but are too massive to be directly produced at present colliders. These particles can appear as virtual contributions that may induce significant effects on branching fractions and angular observables. A review of the present flavour anomalies observed by the LHCb experiment in the context of FCNC processes proceeding through $b \to s\ell^+\ell^-$ transitions is given. The results discussed are obtained from data collected at $\sqrt{s} = 7$ and 8 TeV during Run 1, corresponding to 3 fb^{-1} of integrated luminosity. Results exploiting the data from Run 2 collected at $\sqrt{s} = 13$ TeV and corresponding to 2 fb^{-1} of integrated luminosity, are also included.

Sixth Annual Conference on Large Hadron Collider Physics (LHCP2018)
4-9 June 2018
Bologna, Italy

[*] Speaker.
[†] On behalf of the LHCb collaboration.

PoS(LHCP2018)182

1. Introduction

In flavour physics the underlying dynamics of quark transitions are described in the context of a low-energy effective Hamiltonian ($\mathscr{H}_{eff}$). This is achieved by integrating out heavy degrees of freedom, such as the $W^{\pm}$ and Z bosons and t quark. The resulting $\mathscr{H}_{eff}$ can then be expressed as the sum of local operators (O_i), encoding the dynamics of processes, multiplied by effective couplings (C_i) called Wilson coefficients, describing the strength with which the O_i enter the $\mathscr{H}_{eff}$. For $b \to s\ell^+\ell^-$ transitions, the operators that are of particular importance are $O_{9,10}$, which describe the electroweak penguin and the box diagram contributions [1, 2]. Measurements of $b \to s\ell^+\ell^-$ transitions are typically performed in several bins of dilepton invariant mass squared (q^2). Contributions from dileptons produced close in mass to the J/ψ and $\psi(2S)$ mesons are vetoed from the measurements, while no attempt is usually made to veto or disentangle broad resonances that are present above the $\psi(2S)$ meson.

2. Branching fraction measurements

The LHCb collaboration has performed several measurements of the branching fraction ($\mathscr{B}$) of FCNC exclusive decays using two muons as a final dilepton state, taking advantage of the high performance of the LHCb detector to identify, trigger and reconstruct this type of lepton [3]. A selective collection of $\mathscr{B}$ measurements is illustrated in Figure 1; all $\mathscr{B}$ measurements of the rare (non-resonant) modes are performed relative to their control modes (dilepton pair originating from the J/ψ resonance). The measurements are found to be consistent with the SM predictions, which are heavily influenced by hadronic uncertainties. However, a consistent pattern emerges corresponding to several modest deviations from SM predictions in the low q^2 region, i.e. below 6 GeV^2/c^4, where data are consistently below the predictions [4, 5, 6, 7]. The most significant deviation has been observed in the $\mathscr{B}$ measurement of the $B_s^0 \to \phi\mu^+\mu^-$ decay, where a 3.3 σ discrepancy is observed in the $1.0 < q^2 < 6.0\ \mathrm{GeV}^2/c^4$ region [7].

3. Lepton flavour universality tests

In the SM the ratio of $\mathscr{B}$ of decays that differ only in the flavour of the final state leptons is expected to be unity, except for small deviations that only become important at low q^2 ($\sim 4m_\ell^2$), mainly due to phase-space effects and differences in the coupling of the leptons with the Higgs boson, which depend on the mass of the former. The construction of observables defined as the ratio of $\mathscr{B}$'s of decays with different lepton flavours in their final state, such as:

$$R_K \equiv \frac{\mathscr{B}(B^+ \to K^+\mu^+\mu^-)}{\mathscr{B}(B^+ \to K^+e^+e^-)} \quad \text{and} \quad R_{K^{*0}} \equiv \frac{\mathscr{B}(B^0 \to K^{*0}\mu^+\mu^-)}{\mathscr{B}(B^0 \to K^{*0}e^+e^-)}\ , \tag{3.1}$$

are of particular importance, since theoretical and experimental uncertainties largely cancel at leading order. To further reduce experimental uncertainties, $\mathscr{B}$'s defined in Equation 3.1 are measured as double ratios, where the rare modes are divided by their corresponding control modes, $B^+ \to J/\psi(\to \ell^+\ell^-)K^+$ and $B^0 \to J/\psi(\to \ell^+\ell^-)K^{*0}$ for the R_K and $R_{K^{*0}}$, respectively. The measurement of R_K from LHCb in the q^2 region of $1 < q^2 < 6\ \mathrm{GeV}^2/\mathrm{c}^4$,

$$R_K = 0.745^{+0.090}_{-0.074} \pm 0.036 \tag{3.2}$$

PoS(LHCP2018)182

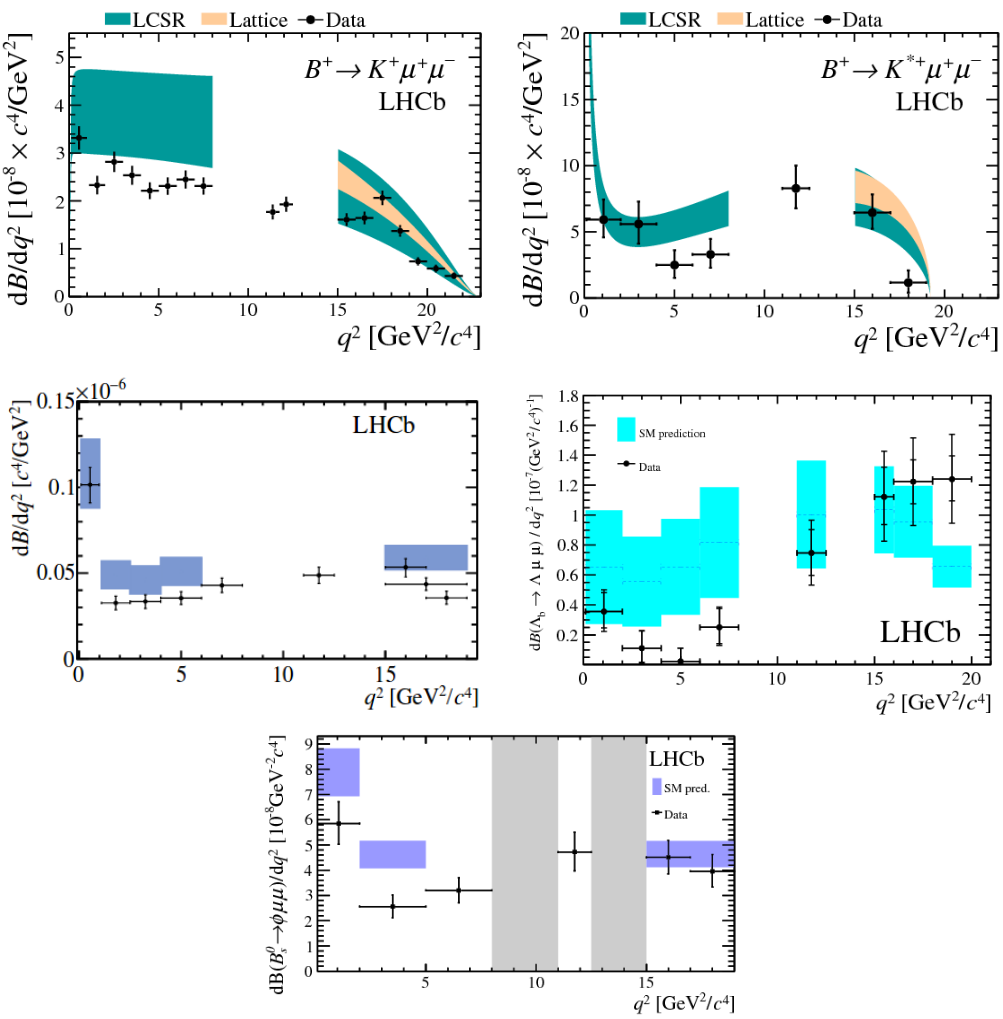

Figure 1: Differential $\mathscr{B}$ measurements using Run 1 data, compared with the SM predictions are illustrated: $B^+ \to K^+\mu^-\mu^+$ [4], $B^+ \to K^{*+}\mu^+\mu^-$ [4], $B^0 \to K^{*0}\mu^+\mu^-$ [5], $\Lambda_b^0 \to \Lambda\mu^+\mu^-$ [6] and $B_s \to \phi\mu^+\mu^-$ [7], where the contributions from the J/ψ and $\psi(2S)$ mesons are veto. Improvements in Lattice QCD calculations of the form factors of the decay of $\Lambda_b^0 \to \Lambda\mu^+\mu^-$ have significantly reduced the uncertainty on the SM prediction of the differential $\mathscr{B}$ [8].

manifests a 2.6 σ deviation with respect to SM predictions [9]. The $R_{K^{*0}}$ ratio is also measured by LHCb,

$$R_{K^{*0}} = \begin{cases} 0.66^{+0.11}_{-0.07} \pm 0.03 \ : \ 0.045 < q^2 < 1.1 \text{ GeV}^2/\text{c}^4 \\ \\ 0.69^{+0.11}_{-0.07} \pm 0.05 \ : \quad 1.1 < q^2 < 6.0 \text{ GeV}^2/\text{c}^4 \end{cases} \tag{3.3}$$

where local deviations of the order of 2.5 σ for each of the two q^2 bins with respect to SM predictions [10] are observed. In Figure 2 the two dimensional distribution of $m(K^+\pi^-\ell^+\ell^-)$ versus q^2 illustrates the difficulties faced in reconstructing the electron mode, with the latter to dominate the uncertainties in the measurements of R_K and $R_{K^{*0}}$.

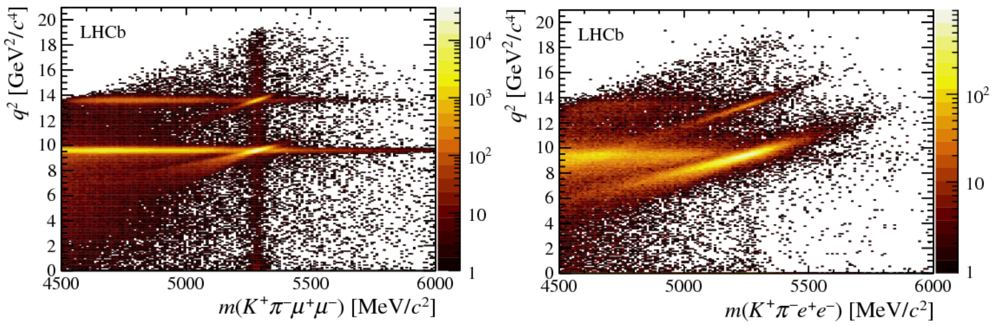

Figure 2: Distribution of $m(K^+\pi^-\ell^+\ell^-)$ versus q^2 reconstructed using $B^0 \to K^+\pi^-\ell^+\ell^-$ candidates, for (left) muons and (right) electrons as a final dilepton states. The low reconstruction efficiency and a much more pronounced Bremsstrahlung radiation of electrons compared to muons are visible.

4. Angular analyses

Angular analyses of rare hadron decays are of particular interest, because the helicity structure of the decay can result in a wealth of observables that provide additional information on $\mathscr{H}_{eff}$, which is not accessible from simple $\mathscr{B}$ measurements.

4.1 Angular analysis of the decay $B^0 \to K^{*0}\mu^+\mu^-$

One of the most notable measurement performed by the LHCb collaboration is the angular analysis of $B^0 \to K^{*0}\mu^+\mu^-$, where the K^{*0} is reconstructed by the subsequent decay to $K^+\pi^-$. The differential decay rate is described by three angles, i.e. θ_l, θ_b and ϕ [12] and a set of angular observables that depend on q^2. Angular observables are extracted by performing an unbinned maximum likelihood fit to the three angles in bins of q^2, where the $m(K^+\pi^-\mu^+\mu^-)$ and $m(K^+\pi^-)$ invariant mass distributions are used to subtract statistically the likelihood contribution of the combinatorial background and better handle the fraction of the S-wave component, respectively. Angular observables are found in general to have good agreement with respect to the SM predictions, however theoretical uncertainties are still significant. A set of optimised parameters, named $P_i^{(\prime)}$ observables, can be constructed where form factors cancel at leading order [11]. These optimised, $P_i^{(\prime)}$, observables are determined by re-parameterising the likelihood fit. Local deviations are observed in P_5' of the order of 3 σ with respect to the SM predictions in the low q^2 regions of $4 < q^2 < 6$ GeV$^2/c^4$ and $6 < q^2 < 8$ GeV$^2/c^4$. The discrepancy observed in P_5' was subsequently confirmed by several collaborations [13, 14, 15, 16]. Measurements of A_{FB} (forward-backward asymmetry of the lepton-side) and P_5' in several bins of q^2 compared with SM predictions are illustrated in Figure 3.

4.2 Angular analysis of the decay $\Lambda_b^0 \to \Lambda\mu^+\mu^-$

Similarly to mesons, baryonic decays can provide a variety of angular observables and help in the understanding of the structure of $\mathscr{H}_{eff}$. The baryonic decay $\Lambda_b^0 \to \Lambda\mu^+\mu^-$, where the Λ cascades to p and π^-, represents a very interesting example. Due to the fact that the Λ_b^0 has spin $\frac{1}{2}$ and the Λ decays weakly, this decay is characterised by different angular observables compared to $B^0 \to K^{*0}\mu^+\mu^-$, giving access to combinations of Wilson coefficients not present in mesonic decays. The differential decay rate of $\Lambda_b^0 \to \Lambda\mu^+\mu^-$ is described by five angles, i.e. θ_l, θ_b, θ, ϕ_l and

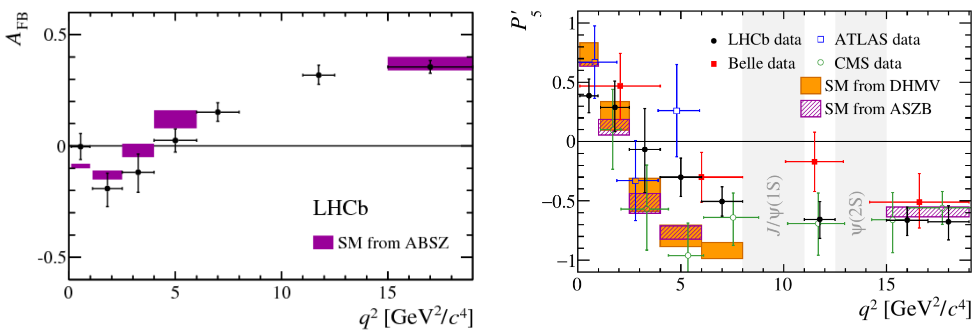

Figure 3: Results of A_{FB} (left) obtained from LHCb collaboration and $P_5^{'}$ obtained from several experiments (right). Theoretical predictions are illustrated with a colored band.

ϕ_b [17] and a set of angular coefficients that exhibit a q^2 dependence. The LHCb collaboration made the first measurements of a limited set of angular coefficients by performing an unbinned maximum likelihood fit in a selected set of one-dimensional angular projections [6]. In order to access the full information of the angular distribution by extracting the compete set of angular observables and relevant correlations, which will allow the measurement to be used in global fits, the previous measurement is updated. The new measurement also includes data from Run 2 corresponding to 2 fb^{-1} of integrated luminosity and in addition uses a moment analysis of the five-dimensional angular distribution to extract the angular observables. This strategy is chosen in order to cope with the significant number of angular observables, given the limited size of the data sample. Results for the forward-backward asymmetries in the lepton-, hadron-side and lepton-hadron are presented: $A^{\ell}_{FB} = -0.39 \pm 0.04 \pm 0.01$, $A^{h}_{FB} = -0.30 \pm 0.05 \pm 0.02$ and $A^{\ell h}_{FB} = 0.25 \pm 0.04 \pm 0.01$, where the one-dimensional angular projections related with the three asymmetry parameters are illustrated in Figure 4. The updated measurement is performed only at low hadronic recoil, corresponding to a q^2 region of $15 < q^2 < 20$ GeV^2/c^4, where the signal contribution is largest. The signal yields are extracted using an unbinned maximum likelihood fit to the invariant mass distribution of $m(p\pi^-\mu^+\mu^-)$, resulting in approximately 600 signal decays; the results of the fits are shown in Figure 5. The measurements of the asymmetries are found to be consistent with the SM predictions, however, a small deviation of the order of 2.6 σ is observed in $A^{\ell h}_{FB}$ [18].

5. Conclusion

Rare decays of b-hadrons allow stringent tests of the SM to be performed, as well as to search for physics beyond the SM that cannot be directly accessed at present colliders. Several measurements performed by the LHCb collaboration manifest interesting deviations with respect to the SM predictions and point to a consistent pattern with high significance, as shown by multiple global fits to the C_i coefficients [19, 20]. By exploiting the full Run 2 data-set, the LHCb collaboration will drive our understanding of these $b \to s\ell^+\ell^-$ anomalies.

References

[1] P. Koppenburg, Z. Dolezal and M. Smizanska. *Rare decays of b hadrons*, *Scholarpedia* **11** (2016) 32643 [arXiv:1606.00999 [hep-ex]]

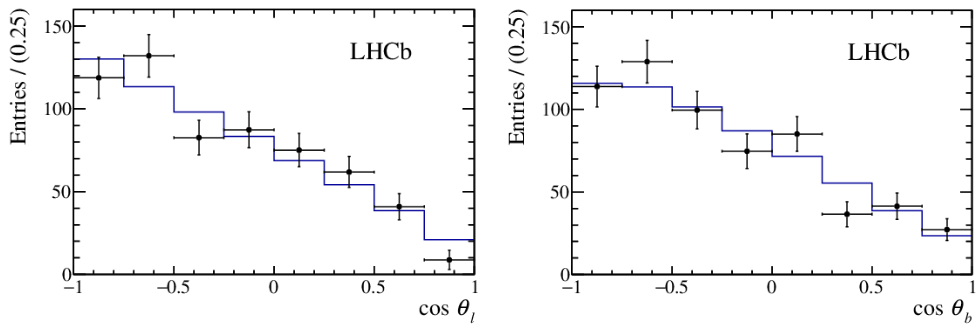

Figure 4: One-dimensional angular projections of $\cos\theta_l$ and $\cos\theta_b$, where θ_l (θ_b) is the polar angle of the positive muon (proton) in the dimuon (Λ) rest frame. The data (dots) includes both data taking-periods and track categories, weighted to correct for background subtraction. The overlaid distribution illustrated by the blue solid line represents the one-dimensional angular distribution, with the angular observables set to values extracted from data, multiplied by the efficiency function [18].

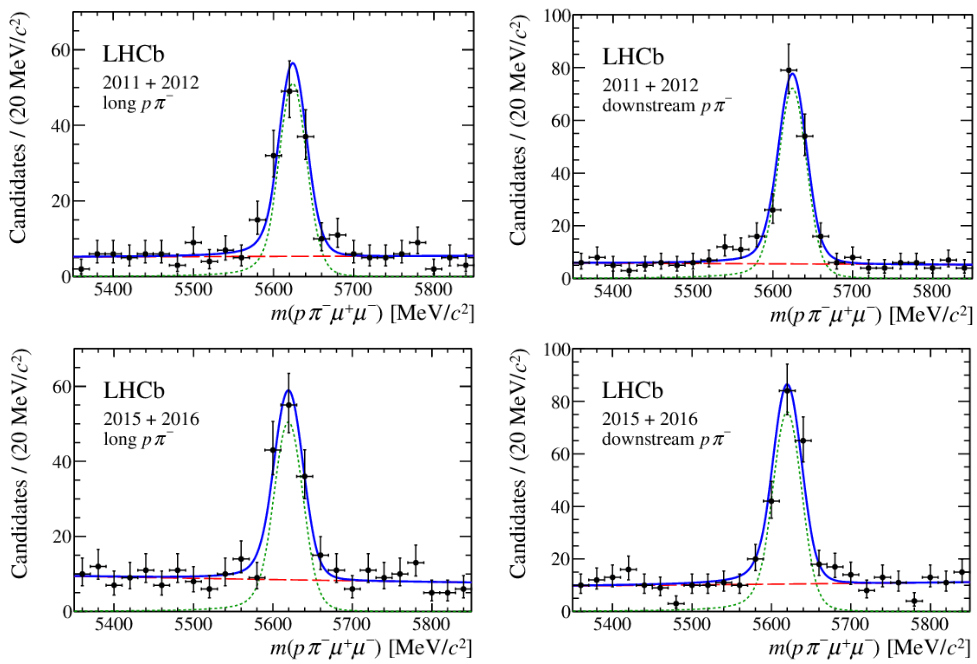

Figure 5: Invariant mass distribution of the $p\pi^-$ system for candidates reconstructed in the long (left) and downstream (right) track categories for the Run 1 (top) and Run 2 (bottom) data-sets. The long (downstream) track category represents candidates where both $p\pi^-$ tracks have (do not have) hits in the VELO [3]. The combinatorial background and signal components of the fit are illustrated by the red dashed and green dotted lines, respectively, while the full fit is illustrated by the blue solid line [18].

[2] G. C. Branco, L. Lavoura, and J. P Silva. *CP Violation*, Int. Ser. Monogr. Phys. **103** (1999) 1, ISBN 978-01987156754

[3] A. A. Alves Jr. et al. *The LHCb detector at the LHC*, *JINST* **3** S08005

[4] R. Aaij et al. *Differential branching fractions and isospin asymmetries of $B \to K^*\mu^+\mu^-$ decays*, *JHEP* **06** (2014) 133 [arXiv:1403.8044 [hep-ex]]

[5] R. Aaij et al. *Measurements of the S-wave fraction in $B^0 \to K^+\pi^-\mu^+\mu^-$ decays and the $B^0 \to K^*(892)^0\mu^+\mu^-$ differential branching fraction*, JHEP **11** (2016) 047. [Erratum: JHEP **04** (2017) 142] [arXiv:1606.04731 [hep-ex]]

[6] R. Aaij et al. *Differential branching fraction and angular analysis of $\Lambda_b^0 \to \Lambda\mu^+\mu^-$ decays*, *JHEP* **06** (2015) 115 [arXiv:1503.07138 [hep-ex]]

[7] R. Aaij et al. *Angular analysis and differential branching fraction of the decay of $B_s \to \phi\mu^+\mu^-$*, JHEP **09** (2015) 179 [arXiv:1506.08777 [hep-ex]]

[8] W. Detmold and S. Meinel. *$\Lambda_b \to \Lambda\ell^+\ell^-$ form factors, differential branching fraction, and angular observables from lattice QCD with relativistic b quarks*, *Phys. Rev.* **D.93** (2016) 074501 [arXiv:1602.01399 [hep-lat]]

[9] R. Aaij et al. *Test of lepton universality using $B^+ \to K^+\ell^+\ell^-$ decays*, *Phys. Rev. Lett* **113** 151601 [arXiv:1406.6482 [hep-ex]]

[10] R. Aaij et al. *Test of lepton universality with $B^0 \to K^{*0}\ell^+\ell^-$ decays*, *JHEP* **08** (2017) 055 [arXiv:1705.05802 [hep-ex]]

[11] S. Descotes-Genon, J. Matias, M. Ramon and J. Virto, *Implications from clean observables for the binned analysis of $B \to K^*\mu^+\mu^-$ at large recoil*, *JHEP* **01** (2013) 048 [arXiv:1207.2753 [hep-ph]]

[12] R. Aaij et al. *Differential branching fraction and angular analysis of the decay $B^0 \to K^{*0}\mu^+\mu^-$*, *JHEP* **08** (2013) 131 [arXiv:1304.6325 [hep-ex]]

[13] R. Aaij et al. *Angular analysis of the $B^0 \to K^{*0}\mu^+\mu^-$ decay using 3 fb^{-1} of integrated luminosity*, *JHEP* **02** (2016) 104 [arXiv:1512.04442 [hep-ex]]

[14] A. M. Sirunyan et al. *Measurement of angular parameters from the decay $\mathrm{B}^0 \to \mathrm{K}^{*0}\mu^+\mu^-$ in proton-proton collisions at $\sqrt{s} = 8$ TeV*, j.physletb.2018.04.030 [arXiv:1710.02846 [hep-ex]]

[15] S. Wehle et al. *Lepton-Flavor-Dependent Angular Analysis of $B \to K^*\ell^+\ell^-$*, *Phys. Rev. Lett.* **118** 111801 [arXiv:1612.05014 [hep-ex]]

[16] ATLAS Collaboration. *Angular analysis of $B_d^0 \to K^*\mu^+\mu^-$ decays in pp collisions at $\sqrt{s} = 8$ TeV with the ATLAS detector*, ATLAS-CONF-2017-023

[17] T. Blake and M. Kreps. *Angular distribution of polarised Λ_b baryons decaying to $\Lambda\ell^+\ell^-$*, *JHEP* **11** (2017) 138 [arXiv:1710.00746 [hep-ph]]

[18] R. Aaij et al. *Angular moments of the decay $\Lambda_b^0 \to \Lambda\mu^+\mu^-$*, [arXiv:1808.00264 [hep-ex]]

[19] B. Capdevila, A. Crivellin, S. Descotes-Genon, J. Matias and J. Virto. *Patterns of New Physics in $b \to s\ell^+\ell^-$ transitions in the light of recent data*, *JHEP* **01** (2018) 093 [arXiv:1704.05340 [hep-ph]]

[20] W. Altmannshofer, P. Stangl and D. M. Straub. *Interpreting Hints for Lepton Flavor Universality Violation*, *Phys. Rev.* **D96** (2017) 055008 [arXiv:1704.05435 [hep-ph]]

PoS(LHCP2018)182